Hydrogen peroxide-assisted photocatalytic water treatment for the removal of anthropogenic trace substances from the effluent of wastewater treatment plants

Tobias Schnabel, Simon Mehling, Jörg Londong and Christian Springer

ABSTRACT

Supported titanium dioxide catalysts were used in a photocatalytic flat cell reactor to remove organic micropollutants from real wastewater. Catalysts based on stainless steel mesh with a porous coating made of titanium dioxide nanoparticles with predominantly anatase modification were used. The influence of the retention time, and light output, and the effect of hydrogen peroxide on the degradation were examined. The kinetics of the degradation of the parent substances was determined by liquid chromatography-tandem mass spectrometry. As a result, first-order degradation kinetics could be confirmed for all substances. The irradiance had no linear influence on the degradation of the compounds. Hydrogen peroxides were added to the wastewater to be treated, as electron acceptors and boosters, and alone had no great oxidative effect on the parent substances. The combination of photocatalysis with the addition of hydrogen peroxide as an electron acceptor had great synergetic effects which can reduce the required energy of the process through a short retention time. The process is suitable for the removal of micropollutants from wastewater.

Key words | anthropogenic micropollutants, hydrogen peroxide, photocatalysis, titan dioxide, UV-A light, wastewater treatment

Tobias Schnabel (corresponding author)
MFPA Weimar – Materials Research and Testing Institute Weimar,
Weimar,
Germany
E-mail: *tobias.schnabel@mfpa.de*

Simon Mehling
Jörg Londong
Department of Civil Engineering, Professorship of Urban Water Management,
Bauhaus-Universität Weimar,
Weimar,
Germany

Christian Springer
Department of Civil Engineering, Professorship Urban Water Management and Environmental Technology,
Erfurt University of Applied Sciences,
Weimar,
Germany

HIGHLIGHTS

- Advanced oxidation processes for the removal of micropollutants.
- Photocatalytic reaction in combination with hydrogen peroxide.
- Fixated photocatalyst out of titan dioxide.

INTRODUCTION

Organic micropollutants, such as pharmaceutical residues, industrial chemicals, or pesticides, are only degraded partially and retained in conventional wastewater treatment plants (Abegglen & Siegrist 2012). Thus, treated wastewater from municipal wastewater treatment plants represents a major input path for organic micropollutants, especially pharmaceutical residues, into the environment (Bergmann *et al.* 2011). For this reason, an additional (further) treatment stage at municipal wastewater treatment plants is necessary to remove or degrade these micropollutants. This is usually arranged following the biological treatment. For advanced wastewater treatment, adsorptive processes using granulated and powdered activated carbon (Salvestrini *et al.* 2020) and oxidation by ozone are currently established as state of the art (Gottschalk *et al.* 2010; Günthert & Rödel 2013). Advanced oxidation processes (AOPs), which use hydroxyl radicals at ambient temperature as oxidants (Wang & Xu 2012), are not yet used in technical systems as a further treatment stage. The advantage of AOPs is the high oxidation strength of the hydroxyl radicals, which, in principle,

doi: 10.2166/wst.2020.481

enables complete mineralization of organic compounds to water, carbon dioxide, and mineral salts (Kisch 2015). During photocatalysis on titanium dioxide, charge separation occurs on the semiconductor through UV-A light (320–400 nm) (Pitre *et al.* 2017). Electron holes and free electrons are formed in the valence band (Equation (1)). The electron holes can form hydroxyl radicals with hydroxide ions or water molecules (Gaya & Abdullah 2008) (Equation (2)):

$$TiO_2 + h_\gamma \rightarrow TiO_2(h^+ + e^-) \quad (1)$$

$$h^+ + OH^- \rightarrow OH\cdot \quad (2)$$

When free electrons in the valence band fall back into the electron holes, heat is released (Equation (3)):

$$h^+ + e^- \rightarrow E_{heat} \quad (3)$$

This reaction, described last, is called recombination. It is undesirable when using photocatalysis because the recombined electron hole can no longer generate a hydroxyl radical. Hydrogen peroxide is able to intercept the free electrons from the valence band and thereby prevent recombination effects. The hydrogen peroxide reacts with the free electrons to form hydroxide ions and hydroxyl radicals as well (Equation (4)) (Bahnemann *et al.* 1991):

$$H_2O_2 + e^- \rightarrow OH^- + OH\cdot \quad (4)$$

Combined application of photocatalysis and hydrogen peroxide has shown synergetic degradation effects for various organic pollutants (Wei *et al.* 1990; Lu *et al.* 1994; Doong & Chang 1997; Cornish *et al.* 2000; Matsuzawa *et al.* 2002; Barakat *et al.* 2005). An application for wastewater purification using a fluidized bed reactor with various combinations of TiO_2 and hydrogen peroxide was described by Kabir *et al.* (2006). However, the degradation of one substance only (phenol) in ultrapure water was investigated experimentally in this study. A possible application as a further treatment stage in wastewater treatment plants would require proof of the degradation performance of a broad spectrum of substances (Eggen *et al.* 2014; Metz & Ingold 2014). In Germany, there are some recommendations to assess the cleaning performance for the application of further treatment stages (Competence Center for Trace Substances NRW 2016; Competence Center for Trace Substances Baden-Württemberg 2018). Here, an 80% reduction in the concentration of indicator substances in relation to the raw wastewater is required. With regard to the selection of these indicator substances, there are various recommendations based on the Swiss methodology, which has been legally valid since 2016 (GSchV 2020). Furthermore, recent studies have shown a great influence of the contained wastewater constituents, especially organic carbon, on the photocatalytic treatment performance (Schnabel 2020). In the scope of this work, the degradation performance of a photocatalytic flat cell reactor for a selection of 14 micropollutants was investigated using real wastewater samples. The degradation of micropollutants by the combined application of carrier-bound photocatalysis and hydrogen peroxide has not yet been investigated in a real wastewater matrix. Inside the reactor, a new type of folded carrier-bound catalyst material was used, which allows a more volume-efficient arrangement of the catalyst surface. The use of UV-A LEDs with a defined energy flux density on the catalyst is also a novel approach. The experiments examined the influence of retention time and irradiation power on substance degradation. In a further step, the combination of photocatalysis and hydrogen peroxide was investigated experimentally.

METHODS

Chemicals and materials

A titanium dioxide-coated stainless steel mesh was used as a catalyst support. The mesh size of the stainless steel mesh was 200 μm with a wire thickness of 100 μm. The fabric is made of V4A high-grade stainless steel (316 L/1.4404). An aqueous nanoparticle suspension made from commercial fumed anatase-modified titanium dioxide nanoparticles between 10.4 and 50 nm in size was used as the coating. The anatase: rutile ratio of the titanium dioxide was 92:8; the BET (Brunauer–Emmett–Teller) surface area of the TiO_2 particles was 91 m^2/g (Siah *et al.* 2016). The aqueous suspension was sprayed onto the heated carrier material (100–200 °C surface temperature). The fast evaporation of the solvent creates a fractal coating structure with a high inner surface (Figure 1). The catalyst material was folded to get a larger catalyst surface area concerning the reactor geometry.

Hydrogen peroxide from the company Carl Roth with a concentration of 90% was used for the experiments with hydrogen peroxide. A terbutryn solution in methanol with a concentration of 10 μg/l was used as the internal standard for analysis. The terbutryn has a purity of 99.5% and was provided by Sigma Aldrich. The following substances in purity for analysis were used: amisulpride,

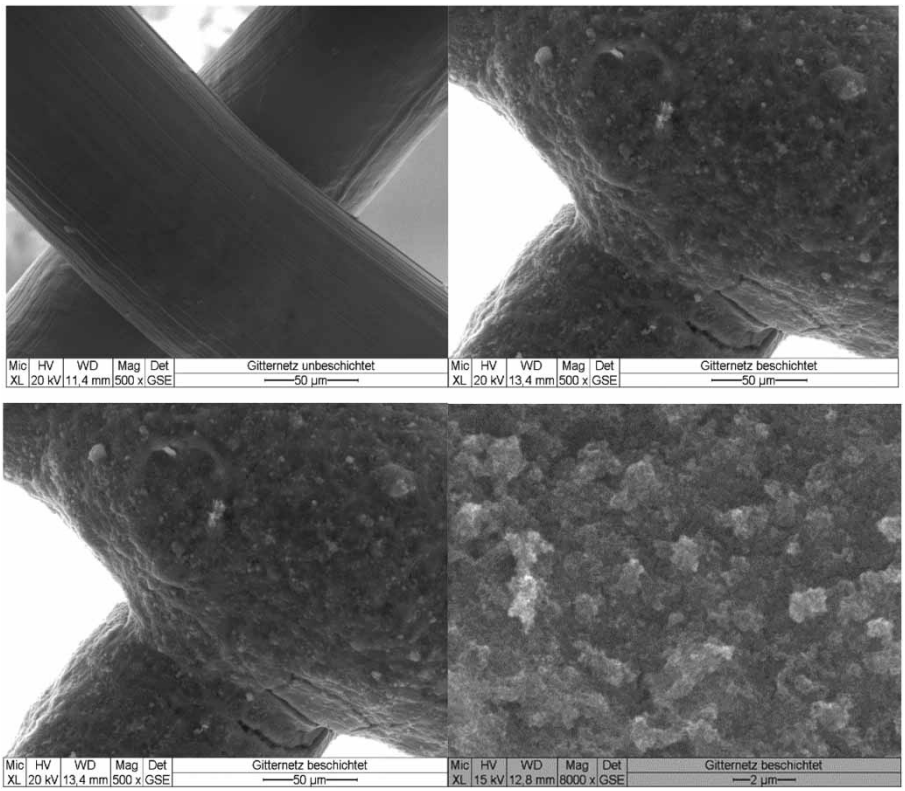

Figure 1 | Scanning electron microscope image of the catalyst surface and non-coated support steel mesh.

benzotriazole, gabapentin, citalopram (Gentham Life Science), carbamazepine, metformin, metoprolol (Sigma Aldrich), 1-methylbenzotriazole, venlaflaxin (Chempure), candesartan (BLD Pharma), diclofenac (Cayman Chemical Company), iopromide (HPC Standards), iohexol (Bayer), iomeprol (Ehrensdorfer).

Experimental set-up and procedure

All tests were performed with effluent samples from the Weimar-Tiefurt wastewater treatment plant. The samples were collected in October 2019 and June 2020. Each wastewater batch was filtered (0.45 µm) and analyzed afterward. All experiments were performed in triplicate. The sole oxidation power of hydrogen peroxide was determined by beaker tests (borosilicate glass). Hydrogen peroxide, 0.1, 0.2, and 0.3 mass-%, was dosed into a 300 ml wastewater solution. The medium was stirred magnetically for 60 minutes at 300 rpm and then sampled.

Figure 2 shows the flat cell reactor, consisting of carrier-bound TiO_2 catalysts and UV-A LEDs (365 nm), in which all photocatalytic experiments were performed. The catalyst was arranged in a stainless steel housing with glass windows

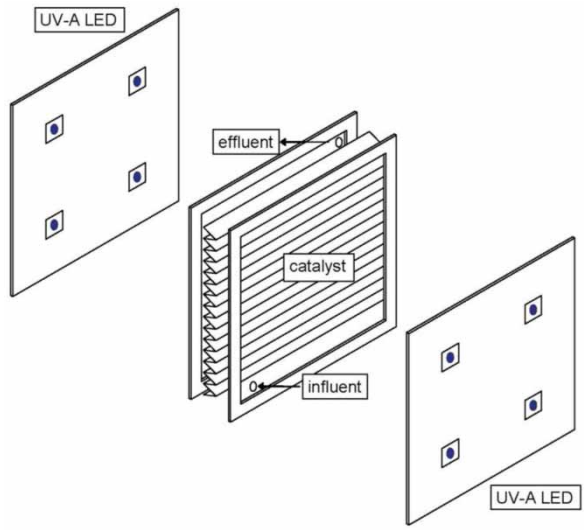

Figure 2 | Schematic representation of the photocatalytic stack reactor.

on the sides and a liquid volume of 200 ml. The catalyst material was a folded stainless steel grid, which was coated with 34 g TiO_2/m^2. The installed catalyst base surface was 128 cm^2. On both sides of the reactor four UV-A LEDs (365 nm) were evenly distributed at a distance of

8 cm. The power could be set via a controllable power supply from 0 to 1.8 W.

The reactor was fed continuously by a peristaltic pump. After an operation time of 10 minutes, which should ensure a continuous operating condition, the reactor effluent was sampled and analyzed. In a first investigation step, the retention time of the reactor at an electrical radiation power of 1.8 W was varied. Retention times of 6 (33.33 ml/min), 8.74 (22.88 ml/min), 11.05 (18.01 ml/min) and 16.71 minutes (11.96 ml/min) were set by adjusting the feed rate accordingly. Subsequently, a series of tests with different irradiation was performed. With a hydraulic retention time of 12.1 minutes (16.43 ml/min), the electrical power of the LEDs was set to 1.44, 1.08, 0.72, and 0.36 W. The combined degradation of pharmaceuticals by photocatalysis and hydrogen peroxide was investigated by dosing hydrogen peroxide to the inlet of the flat cell reactor. Analogous to the degradation tests with H_2O_2 only, dosages of 0.1, 0.2, and 0.3 mass-% were investigated. The flat cell reactor was operated with a residence time of 8.2 minutes (24.42 ml/min) and an irradiation power of 1.8 W.

Analytical methods

The chemical analysis of the trace substances was performed using liquid chromatography tandem mass spectrometry. A Dionex R3000 system with gradient pump and autosampler was used for high-performance liquid chromatography (HPLC). Ultrapure water with 1 mmol/l ammonium acetate and acetonitrile with 0.1% acetic acid was used as the HPLC eluent. A Phenomenex Synergy 2.5 µm hydro PP column measuring 100 × 2 mm was used as the analytical separation column. The flow was 0.25 ml/min and the gradient was run from 4% acetonitrile to 96% acetonitrile in 28 minutes. The injection volume was 100 µl sample, which was mixed with 10 µl internal standard. A Sciex API 4000 triple quadrupole mass spectrometer with electrospray ionization was used for detection. Two multiple reaction monitoring mass transitions were evaluated for each compound. The following substances were analyzed: amisulpride, benzotriazole, candesartan, carbamazepine, citalopram, diclofenac, gabapentin, iopromide, irbesartan, losartan, 1-methylbenzotriazole, metformin, metoprolol, and venlafaxine.

Kinetics and modeling

According to Lin *et al.* (2012) and Ansenjo *et al.* (2013), the kinetics of photocatalytic degradation follows the Langmuir–Hinshelwood (L-H) model. The L-H-model reaction rate can be calculated using Equation (5):

$$r = -\frac{dC}{dt} = k_{LH}\frac{K_L C_{eq}}{1 + K_L C_{eq}} \tag{5}$$

where r is the reaction rate, k_{LH} is the specific rate constant, K_L is the Langmuir constant, and C_{eq} the equilibrium concentration. For the application of the L-H model in photocatalytic wastewater treatment, the presence of reaction products and no related substances must be considered by adding a modified adsorption term (Equation (6)):

$$r = -\frac{dC}{dt} = k_{LH}\frac{K_L C_{eq}}{1 + K_L C_{eq} + \sum_{i=1}^{n} K_i C_i (i = 1, n)} \tag{6}$$

where K_i and C_i are the adsorption constant and concentration of every contained substance at any given time. However, those cannot be measured in real wastewater samples. At low substance concentration, which applies for micropollutants in most wastewater treatment plant effluents, the term $1 + K_L C_{eq} + \sum_{i=1}^{n} K_i C_i (i = 1, n)$ can be neglected and the reaction follows a pseudo-first-order decay rate as described in Equation (7):

$$r = -\frac{dC}{dt} = k_{LH} K_L C_{eq} = k C_{eq} \tag{7}$$

As this is still the subject of ongoing debates, it is necessary to provide experimental evidence when using these kinetics (Lazar *et al.* 2012). In this work, this was achieved by fitting measured normalized concentrations for different hydraulic retention times using Equation (7).

RESULTS

The measured micropollutant concentrations of the effluent at wastewater treatment plant Weimar-Tiefurt are shown in Figure 3. All measured substances were found in each analyzed sample. In all measurements, benzotriazole was present at high concentrations in the range of 6–10 µg/l. Most of the substances were detected in concentrations ranging from 0.5 to 4 µg/l. For some pharmaceuticals (citalopram, irbesartan, losartan, metformin), lower concentration levels were detected. For corrosion inhibitors and X-ray contrast agents (benzotriazole, 1-methylbenzotriazole, iopromide) and some of the pharmaceuticals larger fluctuations in concentration were observed. These pharmaceuticals showed the same patterns of variation.

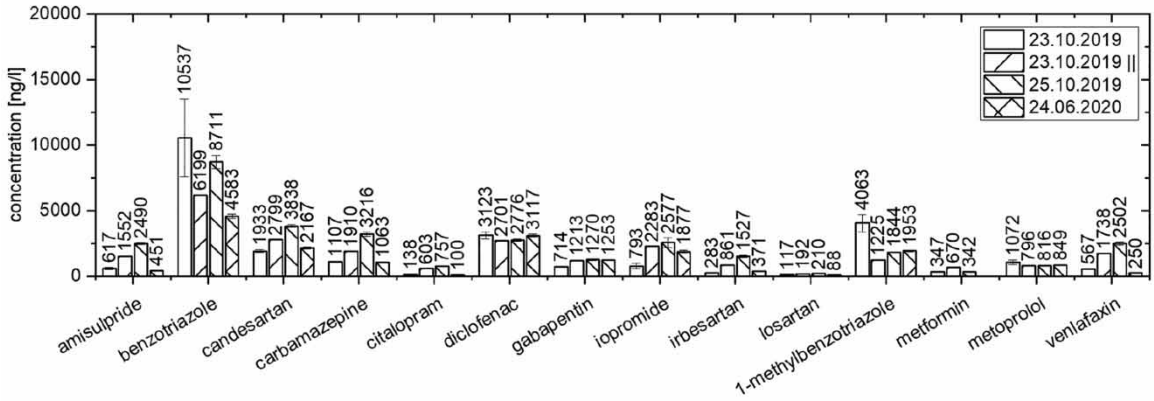

Figure 3 | Concentrations of micropollutants in the sewage treatment plant effluent of Weimar-Tiefurt.

For reasons of clarity, a selection of substances was made for the further description of results. By considering amisulpride, benzotriazole, candesartan, carbamazepine, diclofenac, 1-methybenzotriazole, and metoprolol an assessment of the degradation performance can be made based on existing Swiss legal requirements. As a representative of the poorly degradable X-ray contrast media, iopromide was also included in the further analysis. However, the other substances showed similar behavior in all further experimental steps. A complete compilation of the measurement results can be found in the Appendix.

Figure 4 summarizes the measured influent and effluent concentration of the photocatalytic reactor for different retention times. It shows a significant concentration drop for all shown substances. An increase in retention time was associated with an increase in the degradation rate for all substances. Furthermore, it can be seen that the degree of degradation occurs at a specific level for every micropollutant. Benzotriazole and 1-methylbenzotriazole could be degraded at a high level whereas iopromide was degraded at the lowest rate.

Based on the measured degradation rates as a function of the retention time, reaction constants of a first-order degradation were determined. In Figure 5, fitting curves, reaction constants, and correlation coefficients of the respective substance are summarized. For all micropollutants considered, a very good correlation was achieved (>90%). For a retention time of 6 minutes, a slightly increased degradation rate was measured for amisulpride, benzotriazole, candesartan, carbamazepine, 1-methylbenzotriazole, and metoprolol. It is assumed that this is caused by increased mass transfer caused by turbulence in the reactor system. This shows that the degradation rate approaches a pseudo-first-order reaction rate.

As shown in Figure 6, a reduction in irradiance caused an increase in the measured effluent concentrations for all substances considered. However, for the area-related irradiances of 56–112 W/m^2, this effect was minimal. For

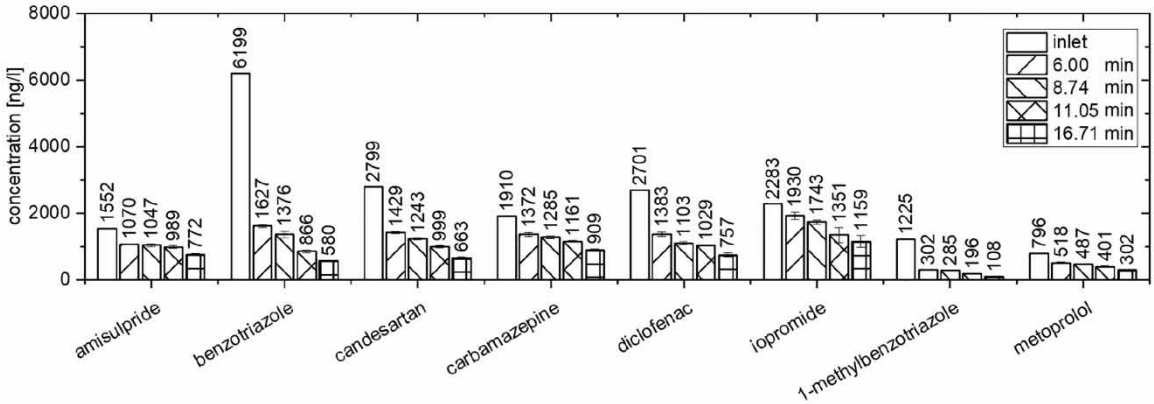

Figure 4 | Photocatalytic degradation with different retention times.

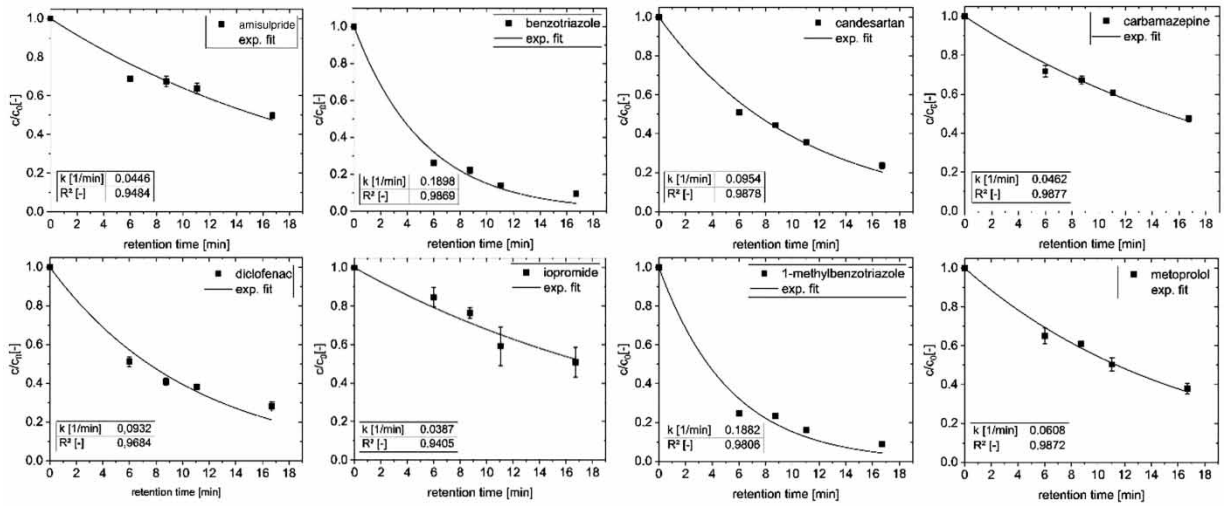

Figure 5 | Exponential degradation kinetics of the eight substances tested.

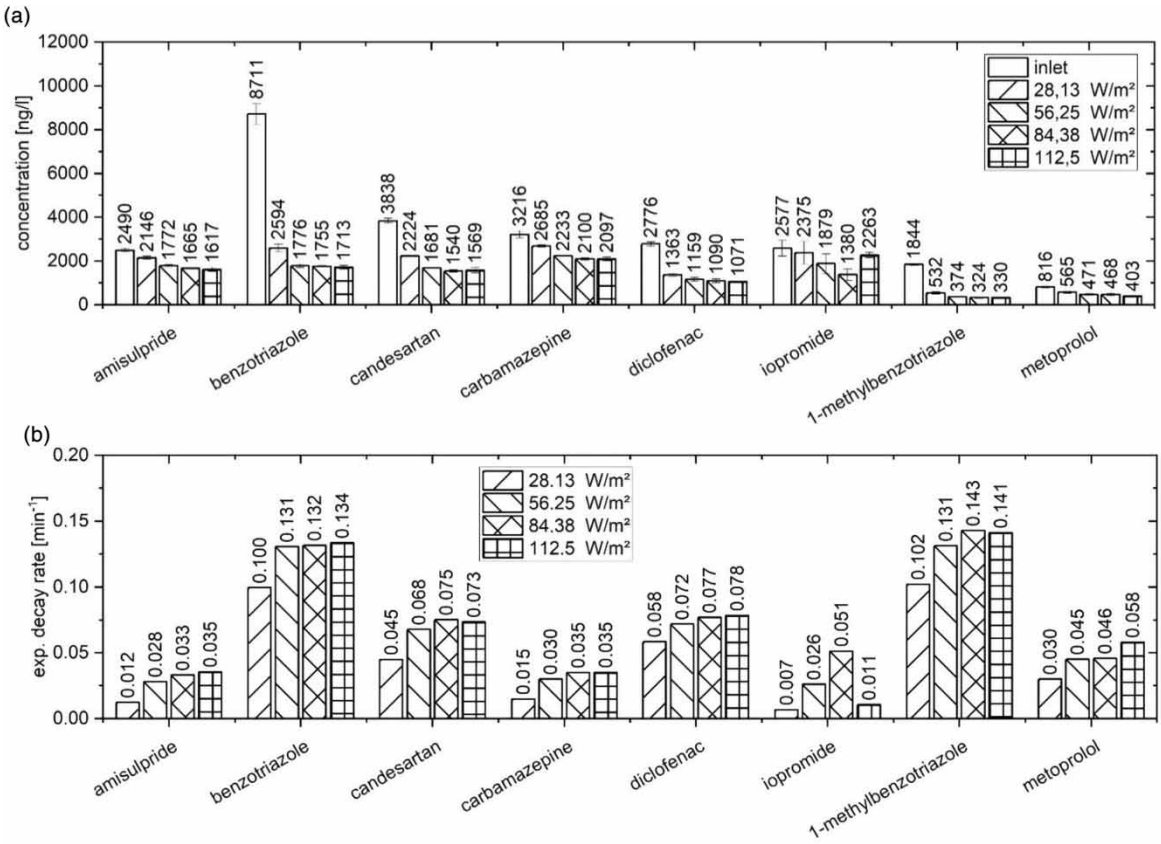

Figure 6 | Measured concentrations (a) and exponential decay rates (b) for photocatalytic degradation with different electrical irradiation energy per base surface.

irradiances of 28 W/m^2, a stronger effect was observed for amisulpride, benzotriazole, candesartan, and carbamazepine. Surprisingly for 112.5 W/m^2, iopromide showed a relatively low degradation rate. It is assumed that this outlier is due to a delay in the continuous operating state caused by comparably poor mass transfer of iopromide

(Durán-Álvarez *et al.* 2020). The degradation constants show a slow non-linear approach to zero with degreasing irradiances. For higher irradiances, the calculated degradation constants approach a maximum value. Especially the degradation constant of diclofenac shows a lower decrease at lower irradiances. The relationship between degradation constant and irradiance is substance-specific. Furthermore, it is shown that further experiments with lower irradiances are necessary for more precise observations of these curves. Exact knowledge of this correlation would enable an energetic optimization of the reactor design. For suspended TiO_2, degradation rates (Kanakaraju *et al.* 2014) of 0.015–0.36 1/min for diclofenac at irradiances of 221.2–484.27 W/m^2 and TiO_2 loadings of 0.01–2.0 g/l in ultrapure water were measured. The measured degradation rates for diclofenac of 0.058–0.078 1/min approach these values very closely at lower irradiances and in the real wastewater matrix.

For the sole H_2O_2-treatment, all analyzed substances showed little to no effects (Figure 7). For the highest H_2O_2-dose benzotriazole, candesartan, diclofenac, and 1-methylbenzotriazole were degraded by about 20% of their initial concentration. The other viewed micropollutants were not oxidized at all. It can be concluded that H_2O_2-treatment alone does not result in a significant reduction in the micropollutant load of sewage treatment plant effluents. Furthermore, for a combined application, it is shown that the photocatalytic reaction is the dominant reaction path. Therefore, according to the shown solo-photocatalysis degradation, the evaluation is made by using first-order reaction kinetics.

By the combined use of hydrogen peroxide within the photocatalytic flat cell reactor, a significant increase in the degradation rate for all viewed substances was achieved (Figure 8). At the lowest H_2O_2-dose tested, amisulpride, candesartan, diclofenac, and iopromide were no longer detectable in the reactor effluent. For the hydrogen peroxide dose of 0.3%, only benzotriazole, 1-methylbenzotriazole and metoprolol were detectable in a low concentration. A comparison of the calculated exponential degradation factors showed a significant increase when photocatalysis and hydrogen peroxide were used in combination versus photocatalysis alone. Because of detection limits exponential degradation factors only could not be calculated for all experimental variants and substances. For amisulpride, carbamazepine, diclofenac, and metoprolol, an increase in the degradation constant by a factor of 4 to 6 was measured. For iopromide, which only showed moderate degradation for sole photocatalytic treatment, a degradation below detection limits was achieved. Benzotriazole and 1-methylbenzotriazole showed a lesser synergistic effect, with degradation rates increasing 1.5 to 3 times. The determined degradation constants of the combined application were only slightly influenced by the dose of hydrogen peroxide used. For the degradation of phenol, Kabir *et al.* (2006) achieved a degradation of 24% after 1 hour by using 50 W/m^2 of irradiation energy and adding 1.07 mg/l of carrier-bound catalysts. Using 1% H_2O_2, degradation could be increased to 33% after 1 hour. For higher doses of hydrogen peroxide, a decrease of phenol degradation was observed for the catalyst concentration above. For a lower catalyst concentration of 0.21 g/l, a phenol degradation of 45% was achieved after 1 hour by adding a 1% dose of H_2O_2. Using suspended TiO_2, a phenol degradation of 18% was achieved at an irradiance of 17 W/m^2 and a TiO_2 concentration of 10 g/l by Barakat *et al.* (2005). By adding $0.5*10^{-3}$ M hydrogen peroxide, the degradation was increased to 78% after 1 hour. A further increase in the hydrogen peroxide dose was accompanied by an increase

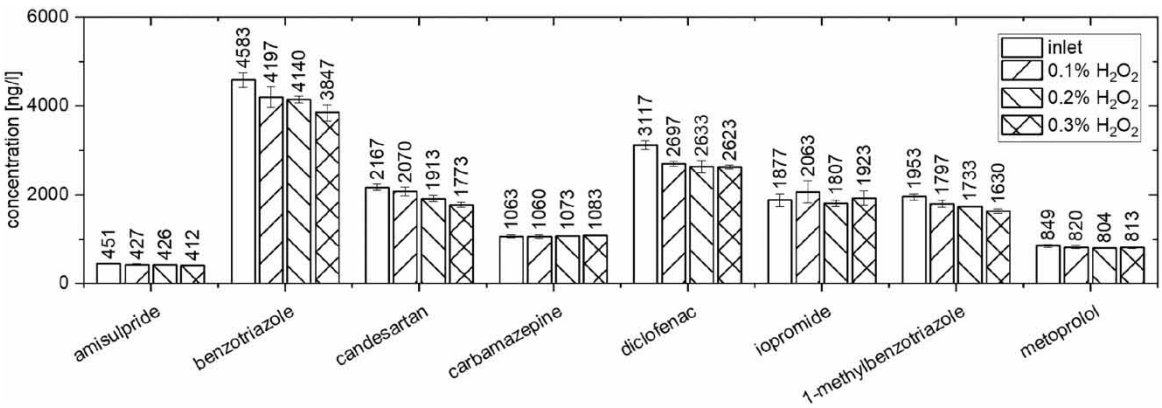

Figure 7 | Degradation of the micropollutants with hydrogen peroxide without photocatalysis.

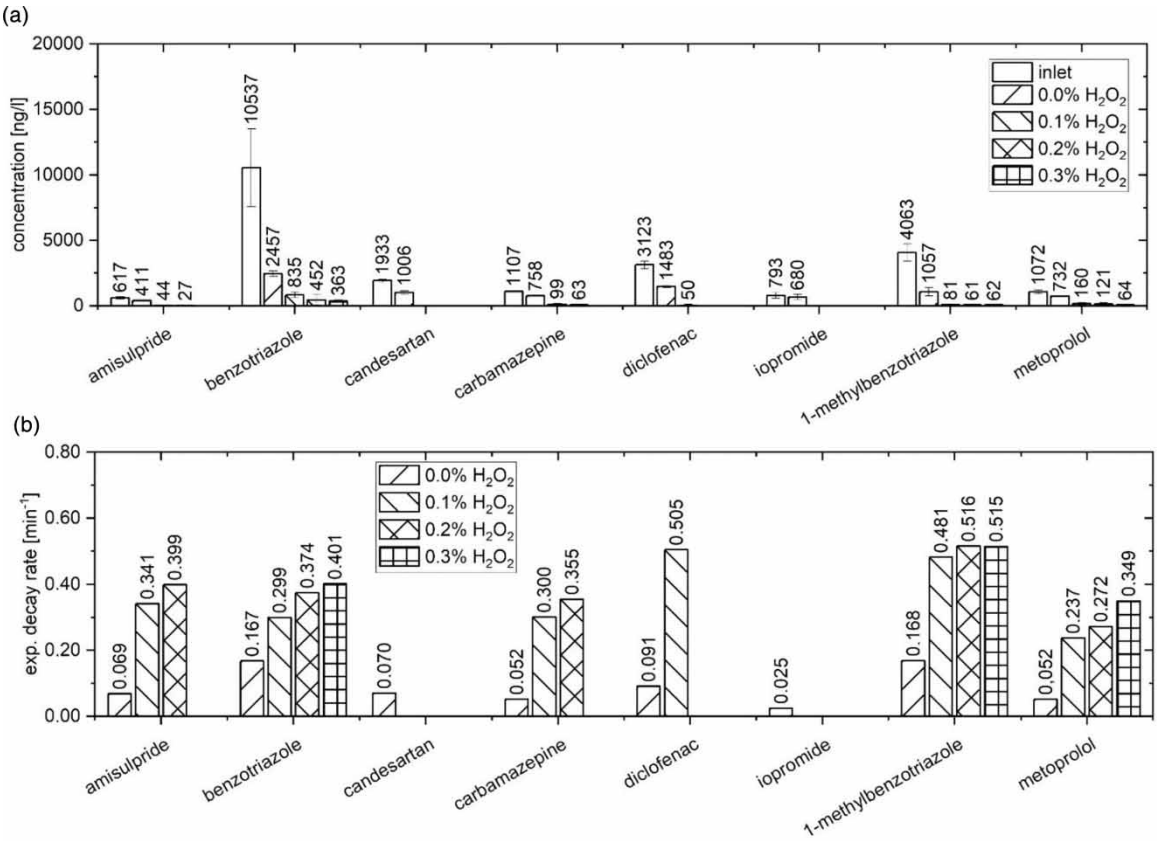

Figure 8 | Measured concentrations (a) and exponential decay rates (b) for combined micropollutant degradation by photocatalysis and hydrogen peroxide.

in phenol degradation. Within both papers, the test was performed using ultrapure water, so that inhibition effects due to wastewater components were not considered. Furthermore, the extent of the measured compounds differs, so that a direct comparison is not possible. In relation to the results in Kabir *et al.* (2006), a significantly better photocatalytic activity of the catalyst material used was found.

CONCLUSIONS

This work aimed to demonstrate the effectiveness of a photocatalytic flat cell reactor as a further treatment stage in a real wastewater matrix. Furthermore, by varying the irradiation power and adding hydrogen peroxide first, optimization approaches were investigated. It could be shown that effective oxidation of micropollutants in a real wastewater matrix can be achieved by carrier-bound photocatalysis. For all investigated substances, a significant reduction in concentration was achieved. A variation of the irradiation power showed a non-linear influence of this parameter on the reaction rate. This offers the possibility of energetic optimization of the reactor system by reducing the area-related radiation power. The novel reactor configuration investigated enables a volume-efficient arrangement of larger catalyst surfaces. By combining photocatalysis and hydrogen peroxide, a strong synergetic effect on the reaction rates of all investigated substances could be observed. For this reaction system, further research is recommended concerning the process parameters irradiation rate and H_2O_2 dose. Although H_2O_2 alone showed a low oxidation power for micropollutants in real wastewater, a consumption of hydrogen peroxide by wastewater constituents is to be expected, especially at lower doses. This effect has to be quantified by additional measurements. Accordingly, appropriate adjustments of the reactor design using the described synergy should be derived. The energy of the methods described within the test series was 0.36–2.5 kWh/m^3. Ozonation in an application as an additional treatment stage has an energy demand of 0.05–0.1 kWh/m^3 (Abegglen & Siegrist 2012). It becomes clear that further energetic optimizations are necessary. However, an exact

calculation of the energy demand of an application of these processes as an additional treatment stage has to be done under consideration of degradation targets as well as the substance-specific elimination rates of the biological treatment stage. There is still a need for research regarding the long-term durability and performance of the catalyst material used. Based on these findings, a final process evaluation can be made on the basis of investment and operating costs. It is known that photocatalytic treatment can achieve complete mineralization of most micropollutants in ultrapure water, but also requires longer treatment times (Kisch 2015). For an application in wastewater, the degradation of transformation products is further slowed by the competition with other wastewater components. Compared to ozonation, photocatalytic applications are expected to result in the reduced formation of transformation products. To what extent harmful transformation products are produced in the application as further treatment stage has to be investigated experimentally. For applications in real wastewater matrices, the use of conventional target analysis is not appropriate. Adapted methods based on non-target and/or biological techniques must be used. Regardless of the oxidative process combination, there is a need for further research on the measurement and quantitative evaluation of transformation products in real wastewater matrices.

DATA AVAILABILITY STATEMENT

All relevant data are included in the paper or its Supplementary Information.

REFERENCES

Abegglen, C. & Siegrist, H. 2012 *Mikroverunreinigungen aus kommunalem Abwasser Verfahren zur weitergehenden Elimination auf Kläranlagen (Micropollutants From Municipal Wastewater Process for Further Elimination in Sewage Treatment Plants)*. Federal Office for the Environment BAFU, Bern, Switzerland.

Ansenjo, N., Santamaria, R., Blanco, C., Granda, M., Alvarez, P. & Menendez, R. 2013 Correct use of the Langmuir–Hinshelwood equation for proving the absence of a synergy effect in the photocatalytic degradation of phenol on a suspended mixture of titania and activated carbon. *Carbon* **55**, 62–69.

Bahnemann, D., Bockelmann, D. & Goslich, R. 1991 Mechanistic studies of water detoxification in illuminated TiO_2 suspensions. *Solar Energy Materials* **24**, 564–583.

Barakat, M. A., Tseng, J. M. & Huang, C. P. 2005 Hydrogen peroxide-assisted photocatalytic oxidation of phenolic compounds. *Applied Catalysis B: Environmental* **59** (1–2), 99–104.

Bergmann, A., Fohrmann, R. & Weber, F.-A. 2011 *Zusammenstellung von Monitoringdaten zu Umweltkonzentrationen von Arzneimitteln. (Compilation of Monitoring Data on Environmental Concentrations of Medicinal Products)*. Federal Environment Agency, Dessau-Roßlau, Germany.

Competence Center for Trace Substances Baden-Württemberg (Ed.) 2018 *Handlungsempfehlungen für die Vergleichskontrolle und den Betrieb von Verfahrenstechniken zur gezielten Spurenstoffelimination. (Recommendations for Action for Comparative Control and the Operation of Process Technologies for Targeted Trace Substance Elimination)*.

Competence Center for Trace Substances. NRW (Ed.) 2016 *Anleitung zur Planung und Dimensionierung von Anlagen zur Mikroschadstoffelimination. (Instructions for Planning and Dimensioning Plants for Micropollutant Removal)*.

Cornish, B. J. P. A., Lawton, L. A. & Robertson, P. K. J. 2000 Hydrogen peroxide enhanced photocatalytic oxidation of microcystin-LR using titanium dioxide. *Applied Catalysis B: Environmental* **25** (1), 59–67.

Doong, R.-a. & Chang, W.-h. 1997 Photoassisted titanium dioxide mediated degradation of organophosphorus pesticides by hydrogen peroxide. *Journal of Photochemistry and Photobiology A: Chemistry* **107** (1–3), 239–244.

Durán-Álvarez, J. C., Hernández-Morales, V. A., Rodríguez-Varela, M., Guerrero-Araque, D., Ramirez-Ortega, D., Castillón, F., Acevedo-Peña, P. & Zanella, R. 2020 Ag_2O/TiO_2 nanostructures for the photocatalytic mineralization of the highly recalcitrant pollutant iopromide in pure and tap water. *Catalysis Today* **341**, 71–81.

Eggen, R. I. L., Hollender, J., Joss, A., Schärer, M. & Stamm, C. 2014 Reducing the discharge of micropollutants in the aquatic environment: the benefits of upgrading wastewater treatment plants. *Environmental Science & Technology* **48** (14), 7683–7689.

Gaya, U. I. & Abdullah, A. H. 2008 Heterogeneous photocatalytic degradation of organic contaminants over titanium dioxide: a review of fundamentals, progress and problems. *Journal of Photochemistry and Photobiology* **9** (1), 1–12.

Gottschalk, C., Libra, J. & Saupe, A. 2010 *Ozonation of Water and Wastewater. A Practical Guide to Understanding Ozone and its Applications*, 2nd edn. Wiley VCH, Weinheim, Germany.

GSchV 2020 Gewässerschutzverordnung (Water Protection Ordinance), 1 January 2020. Switzerland.

Günthert, F. W. & Rödel, S. 2013 *Bewertung Vorhandener Technologien für die Elimination Anthropogener Spurenstoffe auf Kommunalen Kläranlagen. (Assessment of Existing Technologies for the Elimination of Anthropogenic Trace Substances in Municipal Wastewater Treatment Plants. Final Report)*. Abschlussbericht. University of the Bundeswehr. München, Germany.

Kabir, M. F., Vaisman, E., Langford, C. H. & Kantzas, A. 2006 Effects of hydrogen peroxide in a fluidized bed photocatalytic reactor for wastewater purification. *Chemical Engineering Journal* **118** (3), 207–212.

Kanakaraju, D., Glass, B. D. & Oelgemoeller, M. 2014 Titanium dioxide photocatalysis for pharmaceutical wastewater treatment. *Environmental Chemistry Letters* **12**, 27–47.

Kisch, H. 2015 *Semiconductor Photocatalysis: Principles and Applications*. Wiley VCH, Weinheim, Germany.

Lazar, M., Varghese, S. & Nair, S. 2012 Photocatalytic water treatment by titanium dioxide: recent updates. *Catalyst* **2** (4), 572–601.

Lin, Y., Ferronato, C., Deng, N., Wu, F. & Chovelon, J.-M. 2012 Photocatalytic degradation of methylparaben by TiO_2: multivariable experimental design and mechanism. *Applied Catalysis B: Environment* **88** (1–2), 32–41.

Lu, M.-C., Roam, G.-D., Chen, J.-N. & Huang, C.-P. 1994 Photocatalytic oxidation of dichlorvos in the presence of hydrogen peroxide and ferrous ion. *Water Science and Technology* **30** (9), 29–38.

Matsuzawa, S., Tanaka, J., Sato, S. & Ibusuki, T. 2002 Photocatalytic oxidation of dibenzothiophenes in acetonitrile using TiO_2: effect of hydrogen peroxide and ultrasound irradiation. *Journal of Photochemistry and Photobiology A: Chemistry* **149** (1–3), 183–189.

Metz, F. & Ingold, K. 2014 Sustainable wastewater management: is it possible to regulate micropollution in the future by learning from the past? A policy analysis. *Sustainability* **6**, 1992–2012.

Pitre, S., Yoon, T. & Scaiano, T. 2017 Titanium dioxide visible light photocatalysis: surface association enables photocatalysis with visible light irradiation. *Chemical Communications* **53**, S. 4335–S. 4338.

Salvestrini, S., Fenti, A., Chianese, S., Iovino, P. & Musmarra, D. 2020 Diclofenac sorption from synthetic water: kinetic and thermodynamic analysis. *Journal of Environmental Chemical Engineering* **104105**. doi:10.1016/j.jece.2020.104105.

Schnabel 2020 *Photokatalytischer Abbau von Pharmazeutischen Mikroschadstoffen an Trägergebundenen Katalysatoren. (Photocatalytic Degradation of Pharmaceutical Micropollutants on Supported Catalysts)*. Dissertation, Bauhaus-Universität Weimar, Weimar, Germany.

Siah, W., Lintang, H., Shamsuddin, M. & Yuliati, L. 2016 High photocatalytic activity of mixed anatase-rutile phases on commercial TiO_2 nanoparticles. *IOP Conference Series: Materials Science and Engineering* **107**, 012005.

Wang, J. L. & Xu, L. J. 2012 Advanced oxidation processes for wastewater treatment: formation of hydroxyl radical and application. *Environmental Science and Technology* **42** (3), 251–325.

Wei, T.-Y., Wang, Y.-Y. & Wan, C.-C. 1990 Photocatalytic oxidation of phenol in the presence of hydrogen peroxide and titanium dioxide powders. *Journal of Photochemistry and Photobiology A: Chemistry* **55** (1), 115–126.

First received 6 August 2020; accepted in revised form 23 September 2020. Available online 7 October 2020